7. ANKARA INTERNATIONAL AEROSPACE CONFERENCE
11-13 September 2013 - METU, Ankara TURKEY

AIAC-2013-095

COMPUTATIONAL MODELING OF VISCOELASTIC TWO-PHASE SYSTEMS

Daulet Izbassarov[1], Metin Muradoglu[2] and Hadi Nozari[3]
Koc University
Istanbul, Turkey

ABSTRACT

A finite-difference/front-tracking method is developed for the computational modeling of viscoelastic two-phase systems. The method is first validated for the benchmark problem of single phase viscoelastic fluid flow through an axisymmetric channel with a 4:1 contraction and the results are found to compare very well with the computational simulations of Coates et al. (1992). Then it is applied to simulate buoyancy-driven viscoelastic two-phase systems in a capillary tube. Results are in good agreement with the simulations of You et al. (2009). Further simulations are performed to fully characterize the dynamics of buoyancy-driven two-phase viscoelastic systems including a Newtonian droplet in a viscoelastic medium, a viscoelastic droplet in a Newtonian medium and a viscoelastic droplet in another viscoelastic medium for a wide range of rheological properties of phases.

INTRODUCTION

Understanding and modeling of viscoelastic flows is of fundamental importance in polymer and food industries [Owens and Philips, 2005] as well as in modeling of biological fluids [Zhou et al. 2007]. Mathematical models are usually based on the dumbbell assumption and results in highly non-linear system of differential equations. Numerous studies of viscoelastic flows using one or more non-linear differential models with different discretization techniques including finite element, finite difference and finite volume methods can be found in the literature [Bird et al., 1995, Coates et al., 1992, Owens and Philips, 2005]. It has been long recognized that modeling of the viscoelastic effects and the numerical solution of the model equations are a formidable task. In particular, simulations of viscoelastic fluid flows involving free surfaces pose a challenge for numerical methods due to existence of evolving interfaces. The front-tracking method has proven to be a viable tool for simulation of interfacial flows with multi-physics effects and successfully applied to a wide range of multiphase flow problems [Tryggvason et al., 2001; Sarkar and Schowalter, 2000].

This paper presents a front-tracking method developed for the direct numerical simulations of two-phase viscoelastic fluid flows encountered or inspired by micro/biofluidics applications. Two widely used dumbbell models of FENE-CR [Chilcott and Rallison, 1988] and FENE-MCR [Coates et al., 1992] have been incorporated into the front-tracking method. However, it is emphasized here that the numerical method can accommodate other types of complex fluid models such as power-law and Oldroyd-B fluids. The numerical method is first validated for the benchmark single phase and multiphase viscoelastic flows. For this purpose, the method is first applied to the standard single phase viscoelastic fluid flow through an axisymmetric tube with a 4:1 contraction. Then it is validated for the buoyancy-driven two-phase viscoelastic systems including a Newtonian droplet in a viscoelastic fluid and a viscoelastic droplet in a Newtonian fluid. This problem has been recently studied by You et al. (2009). After validating the numerical method for these benchmark single and multiphase flows, extensive simulations are performed to fully characterize the buoyancy-driven two

[1] GRA in a Department of Mechanical Engineering, Email: dizbassarov@ku.edu.tr
[2] Prof. in a Department of Mechanical Engineering, Email: mmuradoglu@ku.edu.tr
[3] GRA in a Department of Mechanical Engineering, Email: hnozari@ku.edu.tr

phase viscoelastic systems including a viscoelastic droplet in another viscoelastic medium, the case not studied by You et al. (2009).

FORMULATION AND NUMERICAL METHOD

The flow is assumed to be incompressible and symmetric about the axis of the tube. Following Unverdi and Tryggvason (1992), one set of governing equations is written for the whole computational domain and different phases are treated as a single fluid with variable material and rheological properties. The interface is tracked explicitly using a Lagrangian grid while the flow equations are solved on a fixed Eulerian grid. The surface tension is computed at the interface using the Lagrangian grid and included into the momentum equation as a body force. The viscoelastic effects are usually accounted for based on the dumbbell models [Owens and Philips, 2005]. In the present study, we consider two such models, namely FENE-CR model of Chilcott and Rallison (1988) and its modified version of FENE-MCR model [Coates et al., 1992]

The continuity and momentum equations are given by

$$\nabla \cdot \boldsymbol{u} = 0, \tag{1}$$

$$\frac{\partial \rho \boldsymbol{u}}{\partial t} + \nabla \cdot (\rho \boldsymbol{u}\boldsymbol{u}) = -\nabla p + \nabla \cdot \mu_s(\nabla \boldsymbol{u} + \nabla \boldsymbol{u}^T) + \nabla \cdot \boldsymbol{\tau} + \int_A \sigma \kappa \boldsymbol{n} \delta(x - x_f) dA, \tag{2}$$

where $\boldsymbol{u}$, p, ρ, μ_s, and $\boldsymbol{\tau}$ are the velocity, the pressure, density, constant solvent viscosity fields and extra stress tensor, respectively. The effects of surface tension is included as a body force in the last term on the right hand side, where σ is the surface tension, κ is twice the mean curvature, and $\boldsymbol{n}$ is a unit vector normal to the interface. The surface tension acts only on the interface as indicated by the three-dimensional delta function δ, whose arguments x and x_f are the points at which the equation is evaluated and a point at the interface, respectively.

The elastic stress tensor $\boldsymbol{\tau}$ is calculated using the FENE-CR model equations, which can be written in terms of a polymer stretch tensor $\boldsymbol{B}$ as [You et al., 2009]

$$\boldsymbol{\tau} = \frac{\mu_p g(\boldsymbol{B})}{\lambda_1} \boldsymbol{B}, \tag{3}$$

$$g(\boldsymbol{B}) = \frac{1}{1 - tr(\boldsymbol{B} + \boldsymbol{I})/L^2}, \tag{4}$$

$$\frac{\lambda_1}{g(\boldsymbol{B})}\left(\frac{\partial \boldsymbol{B}}{\partial t} + \boldsymbol{u} \cdot \nabla \boldsymbol{B} - (\nabla \boldsymbol{u})\boldsymbol{B} - \boldsymbol{B}(\nabla \boldsymbol{u})^T\right) + \boldsymbol{B} = \nabla \boldsymbol{u} + \nabla \boldsymbol{u}^T . \tag{5}$$

FENE-MCR model equations are obtained by substituting the stress tensor for the polymer stretch tensor in Eqs. (3) and (5)

$$\lambda_1\left(\frac{\mathrm{D}}{\mathrm{D}t}\left(\frac{\boldsymbol{\tau}}{g(\boldsymbol{\tau})}\right) - \frac{1}{g(\boldsymbol{\tau})}\left((\nabla \boldsymbol{u})\boldsymbol{\tau} + \boldsymbol{\tau}(\nabla \boldsymbol{u})^T\right)\right) + \boldsymbol{\tau} = \mu_p(\nabla \boldsymbol{u} + \nabla \boldsymbol{u}^T), \tag{6}$$

$$g(\boldsymbol{\tau}) = g(\boldsymbol{B}) = \frac{L^2 + \frac{\lambda_1}{\mu_p} tr(\boldsymbol{\tau})}{L^2 - 3}. \tag{7}$$

When the variation of $\mathrm{D}(1/g(\boldsymbol{\tau}))/\mathrm{D}t$ is neglected, the stress tensor formulation is obtained as

$$\frac{\lambda_1}{g(\boldsymbol{\tau})}\left(\frac{\partial \boldsymbol{\tau}}{\partial t} + \boldsymbol{u} \cdot \nabla \boldsymbol{\tau} - (\nabla \boldsymbol{u})\boldsymbol{\tau} - \boldsymbol{\tau}(\nabla \boldsymbol{u})^T\right) + \boldsymbol{\tau} = \mu_p(\nabla \boldsymbol{u} + \nabla \boldsymbol{u}^T). \tag{8}$$

In Eqs. (3-8) μ_p, λ_1, L, $g(\boldsymbol{\tau})$, tr, $\boldsymbol{B}$ and $\boldsymbol{I}$ are the constant polymeric viscosity fields, the relaxation time, the ratio of the length of a fully extended polymer dumbbell to its equilibrium length, the stretch function, the trace operator, polymer stretch and the identity tensors, respectively. The solvent viscosity ratio is defined as $\beta = \mu_s/\mu_0$, where μ_0 is the zero-shear-rate viscosity given as the sum of solvent and polymeric contributions, $\mu_s + \mu_p = \mu_0$.

It is also assumed that the material properties remain constant following a fluid particle,

$$\frac{\mathrm{D}\rho}{\mathrm{D}t} = 0; \frac{\mathrm{D}\mu_s}{\mathrm{D}t} = 0; \frac{\mathrm{D}\mu_p}{\mathrm{D}t} = 0; \frac{\mathrm{D}\lambda_1}{\mathrm{D}t} = 0, \tag{9}$$

Where $\frac{\mathrm{D}}{\mathrm{D}t} = \frac{\partial}{\partial t} + \boldsymbol{u} \cdot \nabla$ is the material derivative. The density, polymeric and solvent viscosities, and relaxation time vary continuously across the fluid interface and are given by

$$\rho = \rho_i I(r,z,t) + \rho_o\big(1 - I(r,z,t)\big); \quad \mu_p = \mu_{p,i} I(r,z,t) + \mu_{p,o}\big(1 - I(r,z,t)\big);$$

$$\mu_s = \mu_{s,i} I(r,z,t) + \mu_{s,o}\big(1 - I(r,z,t)\big); \quad \lambda_1 = \lambda_{1,\mathrm{i}} I(r,z,t) + \lambda_{1,\mathrm{o}}\big(1 - I(r,z,t)\big) \tag{10}$$

where the subscripts "i" and "o" denote the properties of the drop and bulk fluid, respectively, and $I(r,z,t)$ is the indicator function defined as

$$I(r,z,t) = \begin{cases} 1\ in\ drop\ fluid, \\ 0\ in\ bulk\ fluid. \end{cases} \tag{11}$$

The indicator function is calculated following the procedure described by Tryggvason et al. (2001).

Flow solver

The momentum equations are solved on a stationary staggered nonuniform grid with velocity nodes at the face centers while the pressure, material properties and the extra stress nodes located at the cell centers. The spatial derivatives are approximated using second order central finite-differences for all field quantities. The time integration is achieved using a projection method originally developed by Chorin (1968). The method is briefly described here for completeness. The momentum and mass conservation equations are solved using an operator splitting projection method in two steps. In the first step, the effects of pressure are ignored and the unprojected velocity field is computed as

$$\frac{\rho^{n+1}\boldsymbol{u}^* - (\rho\boldsymbol{u})^n}{\Delta t} = -\nabla\cdot(\rho\boldsymbol{u}\boldsymbol{u})^n + \boldsymbol{F}^n + \mu_s\nabla^2\boldsymbol{u} + \nabla\cdot\boldsymbol{\tau}^n\ . \tag{12}$$

where $\boldsymbol{u}$ is the velocity vector, $\boldsymbol{u}^*$ is the unprojected velocity vector that does not satisfy the mass conservation, the superscript *n* denotes the time step, ∇ is the discrete version of the nabla operator, Δt is the time step, $\boldsymbol{F}^n$ is the body force and the surface tension. In the second step, the velocity is corrected by including the effects of pressure gradient as

$$\frac{\boldsymbol{u}^{n+1} - \boldsymbol{u}^*}{\Delta t} = -\frac{1}{\rho^{n+1}}\nabla p^{n+1}. \tag{13}$$

Taking the divergence of Eq. (13), and requiring that $\boldsymbol{u}^{n+1}$ satisfies continuity, a non-separable Poisson's equation for the pressure field is obtained and is given by

$$\nabla\cdot\left(\frac{1}{\nabla\rho^{n+1}}p^{n+1}\right) = \frac{1}{\Delta t}\nabla\cdot\boldsymbol{u}^*, \tag{14}$$

which is solved on the fixed Eulerian grid using a multigrid method. After obtaining the pressure field from Eq. (14) the velocity field at the new time level is computed as

$$\boldsymbol{u}^{n+1} = \boldsymbol{u}^* - \frac{\Delta t}{\rho^{n+1}}\nabla p\ . \tag{15}$$

In the present paper first order explicit time integration method is used for the time derivatives as described above. However, second order time integration can be easily achieved by a predictor corrector method as described by Tryggvason et al. (2001).

Discretization of the Extra Stress Model Equations

The discretization of the convective term in the extra stress constitutive equations is critically important due to its hyperbolic nature. It is known that central differences results in unphysical oscillations near the sharp gradients in hyperbolic systems. Thus a high resolution scheme utilizing the MINMOD limiter [Harten, 1983] is used to discretize the convective terms in the extra stress equations. The other spatial derivatives are approximated using central differences. A simple explicit Euler method can be used to integrate the model equations in time for a single phase flows. However Euler method or any conventional approximation of the time integration scheme results in singular behavior when passing from the viscoelastic region into Newtonian region as the relaxation time scale λ_1 vanishes in the Newtonian fluid. Sarkar and Schowalter (2000) developed a semi-analytical method to overcome this difficulty and we follow the same procedure as described below.

The FENE-MCR equation for the extra stress can be expressed as:

$$\frac{\lambda_1}{g(\boldsymbol{\tau})}\frac{\partial \boldsymbol{\tau}}{\partial t} + \boldsymbol{\tau} = \boldsymbol{K}(\tau), \tag{16}$$

$$\boldsymbol{K}(t) = \mu_p(\nabla \boldsymbol{u} + \nabla \boldsymbol{u}^T) - \frac{\lambda_1}{g(\boldsymbol{\tau})}(\boldsymbol{u}\cdot\nabla\boldsymbol{\tau} - (\nabla \boldsymbol{u})\boldsymbol{\tau} - \boldsymbol{\tau}(\nabla \boldsymbol{u})^T), \tag{17}$$

where $g(\boldsymbol{\tau})$ is as in Eq. (7). Eq. (16) can be integrated from time t to $t + \Delta t$ to yield

$$\boldsymbol{\tau}^{n+1} = \boldsymbol{\tau}^n e^{-\Delta t g(\boldsymbol{\tau})/\lambda_1} + \boldsymbol{K}(t)\left(1 - e^{-\Delta t g(\boldsymbol{\tau})/\lambda_1}\right). \tag{18}$$

The above scheme is consistent everywhere (including where λ_1=0 for Newtonian case) since the exponential time variation has been retained explicitly. This procedure can be applied to a large class of differential constitutive relations that have the form as in Eq.(16) with the desired result. Furthermore making the approximation $e^{-\Delta t g(\boldsymbol{\tau})/\lambda_1} \cong 1 - \frac{\Delta t g(\boldsymbol{\tau})}{\lambda_1} + O(\Delta t g(\boldsymbol{\tau})/\lambda_1)^2$ and ignoring the higher order terms, Eq. (18) becomes

$$\boldsymbol{\tau}^{n+1} = \boldsymbol{\tau}^n + \frac{\Delta t g(\boldsymbol{\tau})}{\lambda_1}(\boldsymbol{K}(t)^n - \tau^n), \tag{19}$$

which is identical to the explicit Euler method. Note that the same procedure is also used to solve the FENE-CR model equations.

COMPUTATIONAL RESULTS

Single-Phase Viscoelastic Fluid Flow through an Abrupt Axisymmetric 4:1 Contraction

A single-phase viscoelastic fluid flow through an axisymmetric tube with an abrupt 4:1 constriction is considered as shown in Figure 1. The flow conditions are the same as those of Coates et al. (1992). Figure 1 shows the streamlines computed by Coates et al. (1992) (top plots) and the present method (lower plots) for two different Deborah numbers. It is clearly seen from this figure that the present results are in an excellent qualitative agreement with the results of Coates et al. (1992). The asymptotic behavior of the shear stress near the reentrant corner is plotted and compared with the results of Coates et al. (1992) in Figure 2. These two figures show the good quantitative agreement between the present results with the simulations of Coates et al. (1992) for this standard benchmark test case indicating accuracy of the present numerical algorithm.

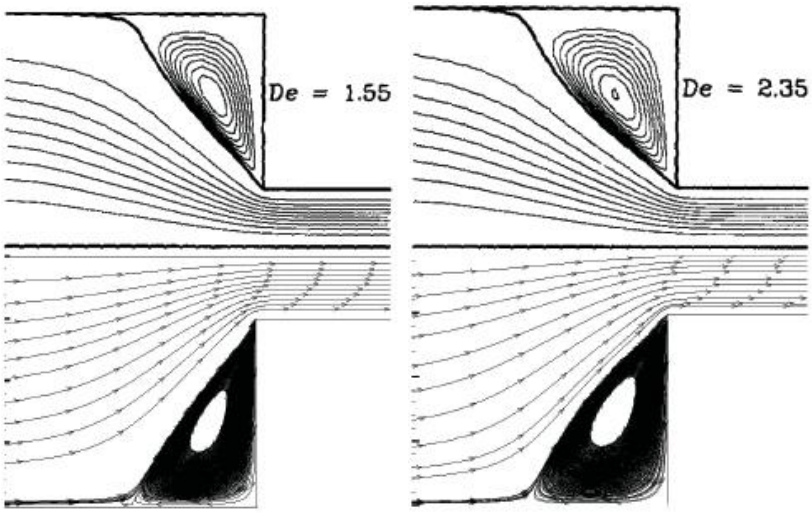

Figure 1: *Corner vortex in calculation on Mesh 6 for the 4:1 contraction with the FENE MCR model at Re = 0.1 and β = 0.01. (top) Coates et al. (1992) data, (bottom) this work.*

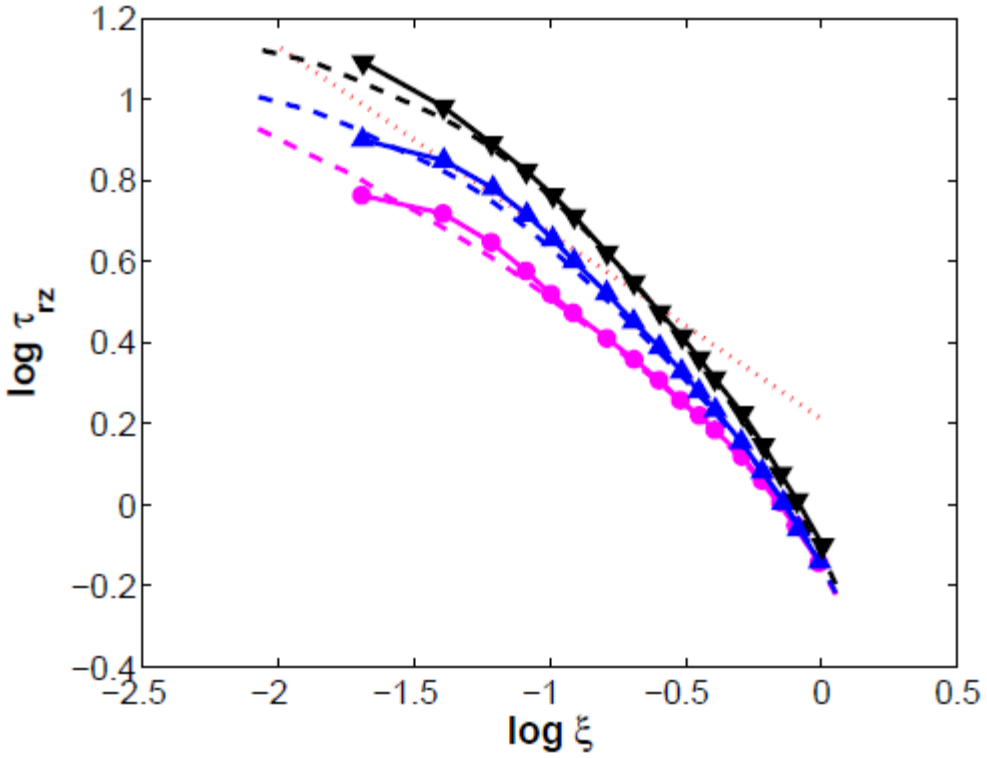

Figure 2: *Asymptotic behavior of the shear stress near the reentrant corner for the FENE-MCR model on finest mesh at Re = 0.1, β = 0.1, De = 0.5(●), De = 1(▲) and De = 2.35(▼). Also presented are values of Coates et al. (1992) (dash-dot lines) with same color for same De.*

Buoyancy-Driven Two-Phase Viscoelastic Systems

Buoyancy-driven two-phase viscoelastic systems are simulated using the present method as a second test case. This problem was recently studied by You et al. (2009) using different numerical method. All three cases of a viscoelastic droplet in a Newtonian medium, a Newtonian droplet in a viscoelastic medium and a viscoelastic droplet in a viscoelastic medium are studied through extensive numerical simulations. The flow conditions are set to be the same as You et al. (2009) to facilitate direct comparisons. The present results are compared with those of You et al. (2009). Note that a viscoelastic droplet in another viscoelastic medium was not studied by You et al. (2009) so only our results are presented for this case. The details of the initial and boundary conditions as well as other flow quantities can be found in You et al. (2009).

A Newtonian Drop Rising in a Viscoelastic Suspending Fluid

The method is first applied to study the motion of a Newtonain droplet rising in a visco-elastic medium. Figure 3 shows a comparison of the present results with the results of You et al. (2009). Figure 3a shows the steady shape of the droplet while Figure 3b shows the steady state distribution of the polymer conformation tensor, **B**. As stated in You et al. (2009), the contours of $\mathbf{B}_{zz}$ show concentrated uniaxial polymer stretch in the region around the rear stagnation point of the drop, which pulls the interface out and results in a tapered trailing end. Since $\mathbf{B}_{zz}$ is small around the leading edge, the drop does not experience noticeable deformation in the vicinity of its front end. The results obtained in this work are overall in good agreements with the study of You et al. (2009) demonstrating the accuracy of the present simulations.

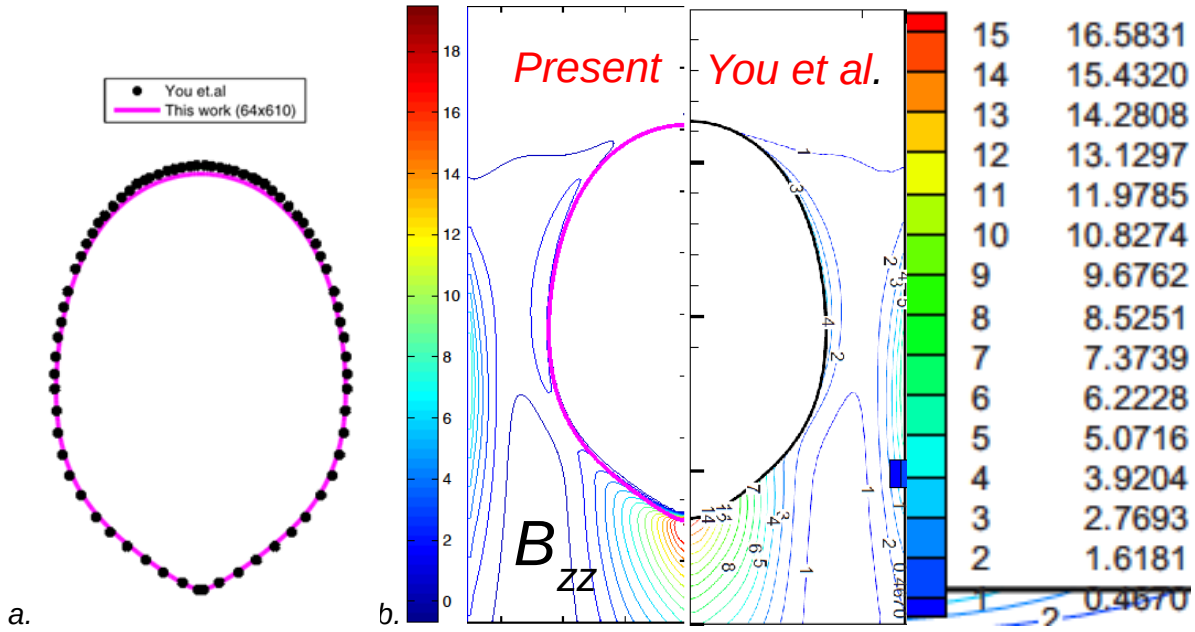

Figure 3: *Comparison of a) droplet front and, b) contours of polymer stretch tensor component for a Newtonian drop rising in a FENE-CR model fluid. Re =10, Ca=20, De=50*

A Viscoelastic Drop Rising in a Newtonian Suspending Fluid

Next a viscoelastic droplet rising in a Newtonian medium is simulated. Figures 4a and 4b show steady state shape of the droplet and the distribution of the polymer conformation tensor component $\mathbf{B_{zz}}$ together with the corresponding results of You et al. (2009). As stated in You et al. (2009), the polymer inside the drop is stretched along the flow direction and the drop achieves a steady cylindrical shape with a dimpled trailing end. Since the local flow direction is normal to the interface at the rear stagnation point, the polymer stretch component $\mathbf{B_{zz}}$ reaches its maximum value at that point and pulls the interface inward. As shown in the Figure 4, the same phenomenon is well captured in the present results being in a good agreement with You et al. (2009).

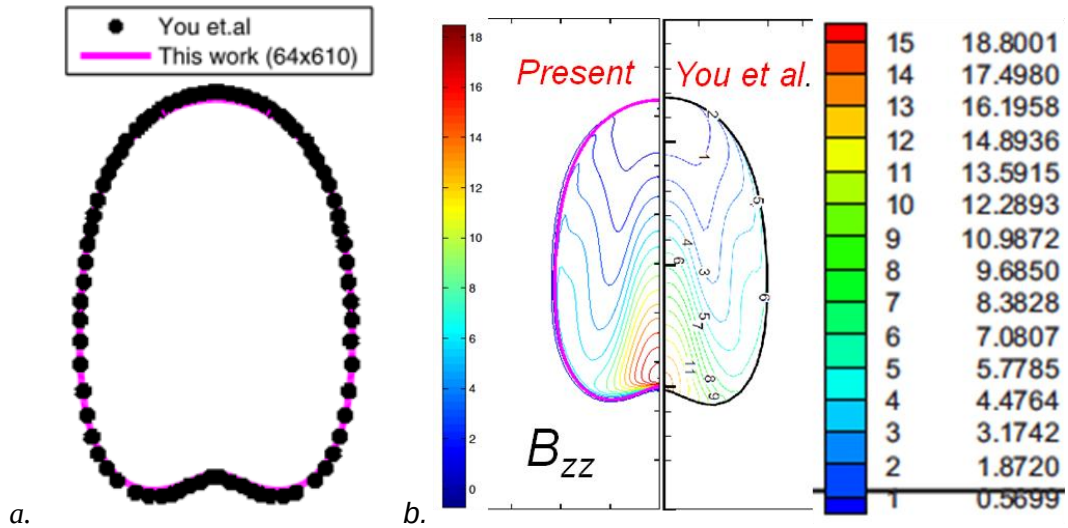

Figure 4: *Comparison of a) droplet front and, b) contours of polymer stretch tensor component for a drop of FENE-CR model fluid rising in a Newtonian suspending fluid. Re =10, Ca =50, De=50*

A Viscoelastic Drop Rising in another Viscoelastic Medium

Finally the buoyancy-driven motion of a viscoelastic droplet rising in another viscoelastic medium is studied. Sample results for this case are shown in Figures 5 and 6. It is observed that shape of the drop depends on the ratio of relaxation times ($\gamma = \frac{\lambda_i}{\lambda_o}$) of the drop and the suspending medium. For $\gamma = 0.2$ prolonged tail is observed. In this case, the relaxation time of medium is 5 times greater than drop, which is similar to the case where Newtonian drop moving in the viscoelastic medium. On the other hand, for $\gamma = 5$, the relaxation time of the drop is 5 times greater than the medium. In this case, the shape of the drop is similar to the case where viscoelastic drop is in Newtonian medium but without any dimple at the trailing end.

Figure 5: *Dependance of a FENE-CR viscoelastic droplet shape in a viscoelastic medium to the ratio of relaxation parameter*

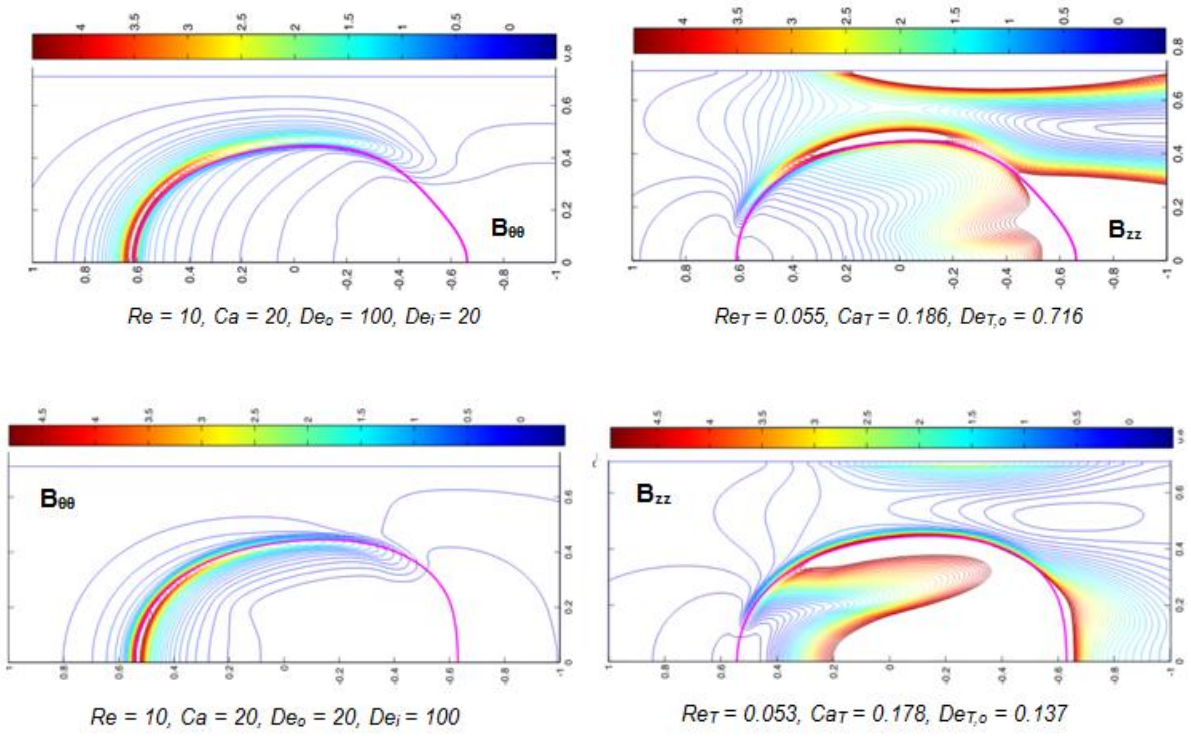

Figure 6: *Contours of velocity and polymer stretch tensor component for a drop of FENE-CR model fluid rising in a Newtonian suspending fluid with relaxation ratio $\gamma = 0.2$ (upper plots) and $\gamma = 5$ (lower plots)*

CONCLUSIONS

A front-tracking method is developed for computations of viscoelastic interfacial flows. The method is validated for single phase and multiphase cases. In single phase case there is a good agreement with the analytical solutions and numerical results of Coates et al. (1992). For multiphase case, the results for Newtonian droplet in viscoelastic medium and viscoelastic droplet in Newtonian medium are in good agreement with the numerical simulations of You et al. (2009). Additionally, the simulations of the dynamics of a viscoelastic droplet in another viscoelastic medium are also presented. As a future study, the numerical method will be applied to study the motion and deformation of a viscoelastic droplet in a pressure driven axisymmetric contraction/expansion micro-channel and the results will be compared with the available numerical and experimental data.

Acknowledgments

The authors are grateful to the Scientific and Technical Research Council of Turkey (TUBITAK) for support of this research through Grant 112M181.

REFERENCES

Bird, R.B. and Wiest, J.M. (1995) Constitutive equations for polymeric liquids, Ann. Rev. Fluid Mech., 27:169-193,1995

Chilcott, M. D. and Rallison, J. M. (1988) Creeping flow of dilute polymer solutions past cylinders and spheres J. Non-Newtonian Fluid Mech., 29:381-432, 1988

Coates, P.J., Armstrong, R.C. and Brown, R.A. (1992) Calculation of steady-state viscoelastic flow through axisymmetric contractions with the EEME formulation J. Non-Newtonian Fluid Mech. 42, 141188., 1992

Owens, R.G. and Phillips, T.N. (2005) Computational Rheology, Imperial College Press, 2005

Muniz, A.R., Secchi, A.R. and Cardozo, N.S.M. (2008) High-order finite volume method for solving viscoelastic fluid flows Braz. J. Chem. Eng. 25, 5358, 2008

Sarkar, K. and Schowalter, W. R. (2000) Deformation of a two-dimensional viscoelastic drop at non-zero Reynolds number in time-periodic extensional flows J. Non-Newtonian Fluid Mech., 95:315-342, 2000

Tryggvason, G., Bunner, B., Esmaeeli, A., Juric, D., Al-Rawahi, N., Tauber, W., et al. (2001) A front-tracking method for the computations of multiphase flow. J. Comput. Phys.169:708, 2001

Unverdi, S.O. and Tryggvason, G. (1992) A front-tracking method for viscous, incompressible, multi-fluid flows J. Comput. Phys. 100(1) p:25-37, 1992

You, R., Haj-Hariri, H. and Borhan, A. (2009) Confined drop motion in viscoelastic two-phase systems Phys. Fluids, 21, Art. No. 013102, 2009

Zhou, C., Yue, P. and Feng, J. (2007) Simulation of Neutrophil Deformation and Transport in Capillaries using Newtonian and Viscoelastic Drop Models, Annals of Biomedical Engineering, Vol. 35, No. 5, May 2007